

Isoform-Specific PKA Dynamics Revealed by Dye-Triggered Aggregation and DAKAP1 α -Mediated Localization in Living Cells

Brent R. Martin,¹ Thomas J. Deerinck,^{2,3} Mark H. Ellisman,^{2,3} Susan S. Taylor,^{1,4,5} and Roger Y. Tsien^{1,4,5,*}

¹Department of Pharmacology

²Department of Neuroscience

³National Center for Microscopy and Imaging Research

⁴Department of Chemistry and Biochemistry

⁵Howard Hughes Medical Institute

University of California, San Diego, 9500 Gilman Drive, La Jolla, CA 92093, USA

*Correspondence: rtsien@ucsd.edu

DOI 10.1016/j.chembiol.2007.07.017

SUMMARY

The tetracysteine sequence YRECCPGCCMWR fused to the N terminus of green fluorescent protein (GFP) self-aggregates upon biarsenical labeling in living cells or in vitro. Such dye-triggered aggregates form temperature-dependent morphologies and are dispersed by photobleaching. Fusion of the biarsenical aggregating GFP to the regulatory (R) or catalytic (C) subunit of PKA traps intact holoenzyme in compact fluorescent puncta upon biarsenical labeling. Contrary to the classical model of PKA activation, elevated cAMP does not allow RI α and C α to diffuse far apart unless the pseudosubstrate inhibitor PKI or locally concentrated substrate is coexpressed. However, RII α releases C α upon elevated cAMP alone, dependent on autophosphorylation of the RII α inhibitory domain. DAKAP1 α overexpression induced R and C outer mitochondrial colocalization and showed similar regulation. Overall, effective separation of type I PKA is substrate dependent, whereas type II PKA dissociation relies on autophosphorylation.

INTRODUCTION

Protein kinase A (PKA) is essential for the regulation of diverse cellular processes, including ion channel conductance, metabolism, cell migration, and gene expression. Decades of research have elucidated many of the biological roles and unique properties of this prototypical kinase, yet recent evidence suggests that the classical mechanism of cAMP-induced dissociation and activation may require revision when explored in a cellular environment [1].

PKA holoenzyme is present as two isoforms in cells, type I and type II, which are defined by the subtype of reg-

ulatory subunit, either RI or RII. Type II holoenzyme preferentially binds many A kinase-anchoring proteins (AKAPs) [2], spatially localizing the holoenzyme to precise subcellular locations or near specific substrates. Whereas RII anchoring is generally static, anchoring of RI to AKAPs is more dynamic. Both RI and RII isoforms bind to C through specific interactions that include docking of an inhibitory peptide into the kinase active site [3]. Phosphorylation of serine at the phosphorylation site (P site) within the RII inhibitory domain decreases the binding affinity of type II PKA holoenzyme [4] and enhances dissociation. The corresponding position of RI is alanine. Although PKA has been thoroughly studied in vitro, it has been technically difficult to monitor the full dissociation of PKA in living cells.

The original evidence that cAMP induces PKA holoenzyme dissociation is based on decades-old chromatography experiments on dilute purified components [4–6]. We have previously shown in cells that cAMP can dissociate fluorescein-labeled C from rhodamine-labeled RI [7] or RII [8] as well as fluorescent protein fusions of C and RII [9], as evidenced by decreases in fluorescent resonance energy transfer (FRET) and migration of C subunit into the nucleus, leaving R in the cytosol. However, random or site-specific chemical labeling of PKA subunits can alter the affinity of holoenzyme and dissociation dynamics (unpublished data), so such modified subunits may fail to reflect endogenous PKA dissociation, even while remaining usable for measuring cAMP. Interestingly, cAMP-evoked decreases in FRET are generally larger with type II holoenzyme than type I [8, 9], which were assumed to be a reflection of the difference in distance and orientation of the two fluorophores in the different PKA isoforms in unstimulated cells. Although dissociation is not required for a FRET change, if dissociation does occur, it reduces FRET all the way to zero, thus providing an additional and more powerful mechanism for FRET reduction than just a conformational readjustment. Recently, cAMP-dependent conformational changes in type I and II PKA have been measured using bioluminescent resonance energy transfer (BRET), although this method sacrifices

single-cell resolution [10]. In cells, cAMP and agonist analogs caused much smaller decreases in BRET in type I than in type II PKA. Time-resolved anisotropy of fluorescently labeled RII α and C α suggested that cAMP-bound holoenzyme is stable yet catalytically active [11]. Unfortunately, kinase activity and dissociation were not simultaneously measured, so the existence of an active intact holoenzyme is still controversial. Small-angle scattering has also verified a stable cAMP-bound form of type I PKA holoenzyme [12]. Despite the circumstantial evidence, intact cAMP-bound PKA holoenzyme has not been visualized in living cells.

During our efforts to optimize the fluorescence and affinity of the biarsenical tetracysteine system, we inadvertently discovered a specific tetracysteine-green fluorescent protein (GFP) that aggregated upon addition of the biarsenical dye ReAsH [13]. We now characterize the structural requirements for such aggregation in greater detail, then apply this system to study PKA dynamics in cells. By inducing colocalization of diffuse PKA holoenzyme, weak interactions between R and C subunits are trapped in highly visible puncta, providing a simple assay to study the mechanisms of C dissociation. The presence or absence of C α in puncta reveals unique differences in the dissociation of type I and type II holoenzyme in living cells, leading to a new cellular understanding of PKA regulation. Furthermore, by DAKAP1 α tethering, the effects of substrate concentration and C α diffusion are correlated with PKA activity in live cells. This reversible system for induced protein colocalization and inactivation opens many opportunities to manipulate complex signaling pathways in living cells.

RESULTS

Biarsenical Dye-Triggered Aggregation of a Tetracysteine-GFP

During mammalian cell-based selections for tetracysteine sequences with enhanced ReAsH brightness and affinity while fused to the N terminus of Emerald GFP [14] with an additional V163A mutation to improve folding, the tetracysteine sequence YRECCPGCCMWR was serendipitously isolated and found to undergo self-aggregation when labeled with ReAsH (Figure 1A; see Movie S1 in the Supplemental Data available with this article online). This tetracysteine-GFP fusion is hereafter referred to as BA-GFP for biarsenical aggregating GFP. By forming insoluble protein aggregates upon labeling, ReAsH-BA-GFP shields itself from high-dithiol washes. Additionally, due to the highly compact nature of the aggregates, FRET from GFP to ReAsH was very efficient, mediated by intermolecular FRET within coaggregated dye complexes. Because fluorescence-activated cell sorting (FACS) ignores subcellular localization, this particular sequence became highly enriched, representing the majority of clones by the final round of selection. Clearly the aggregates were not any more harmful than normal biarsenical labeling, as cells expressing high levels of the tag survived repeated rounds of ReAsH-induced aggregation

and selection during several weeks in culture. BA-GFP clones eventually outcompeted other TC-GFP variants to dominate the final selection pool.

Aggregation occurs shortly after labeling with ReAsH or with the blue fluorescent analog CHOxAsH [15], but not with the green fluorescent analog FIAsh [16] (Figure S1), whose protruding carboxyphenyl ring presumably blocks aggregation. To further understand the requirements for induced aggregation, the tetracysteine was separated from GFP and fused to the N terminus of β -actin and α -tubulin. Both cytoskeletal proteins expressed and localized appropriately in cells and labeled efficiently with ReAsH, but failed to aggregate (Figure S2A). When the complete tetracysteine-GFP tag was fused to the N terminus in a similar manner, aggregation of nonpolymerized β -actin or α -tubulin subunits occurred, but cells failed to retract and the cytoskeleton remained intact (Figure S2B), which could be due to the high levels of endogenous expression. Additionally, swapping the tetracysteine fusion to the C terminus of GFP prevented aggregation (Figure S3A). Fusion of small epitope tags, such as HA or Myc, N-terminal to the tetracysteine in BA-GFP did not disrupt aggregation, but the FLAG epitope or larger protein fusions were inhibitory (Figures S3B and S3C). Clearly, both N-terminal fusion to GFP and an unconstrained tetracysteine N terminus are important for inducible aggregation.

Replacement of Emerald GFP (F64L, S65T, S72A, N149K, M153T, V163A, I167T) with enhanced GFP (F64L, S65T) plus the folding mutation V163A (Figures S4A and S4B) or mutation of the critical residue for chromophore formation, Y66A, drastically increased the critical concentration for aggregation from a few micromolar to near millimolar concentrations inside cells. Fusion to mGFP (F64L, S65T, S72A, N149K, M153T, V163A, I167T, plus the monomerizing mutation A206K) [17] had only a slight effect on the critical concentration (Figures S4A and S4B), whereas fusions to either CFP or YFP lost all ability to aggregate (Figure S3A). Therefore, we chose to use BA-GFP including A206K (BA-mGFP) for further experiments. Purified BA-GFP protein also aggregated upon ReAsH or CHOxAsH labeling in vitro, demonstrating cellular factors are not required for aggregation. Salt removal or 1% SDS dissolved the in vitro precipitates, but the nonionic detergent NP-40 (1%) had no effect. Alanine scanning across six residues flanking the CCPGCC (Y₁R₂E₃-CCPGCC-M₁₀W₁₁R₁₂) implied each residue except R₂ is important for aggregation in cells (Figures S4C and S4D). In summary, aggregation requires a tetracysteine-GFP fusion nearly identical to that originally isolated by FACS selection.

Temperature and Light Control of Aggregation

Depending on the biarsenical labeling temperature, different aggregate morphologies form in living cells. Room temperature labeling promotes the formation of punctate aggregates (Figure 1B) with limited diffusibility from the nucleation site. Alternatively, labeling at 37°C causes formation of fiber-like aggregates, which often coalesce into

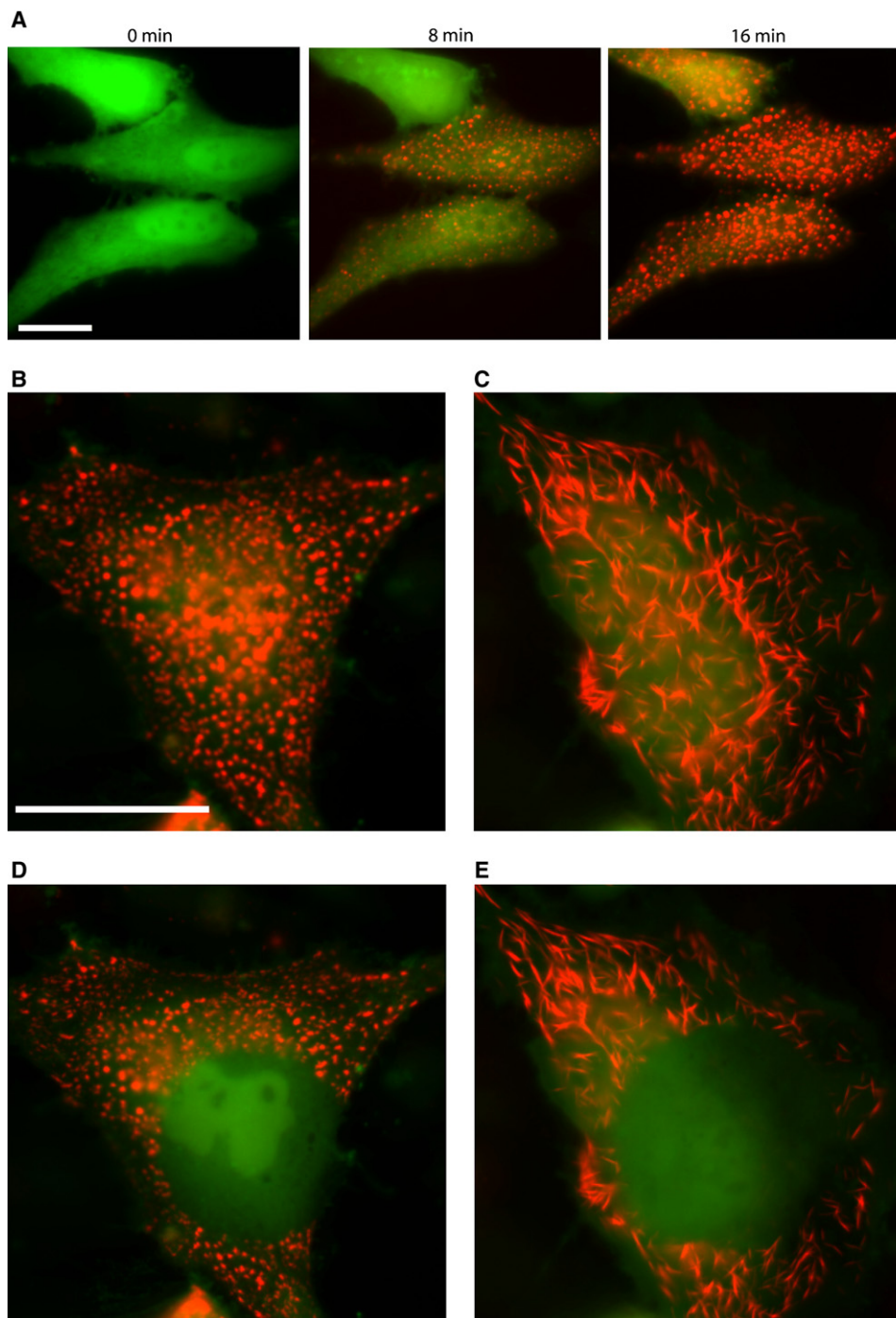


Figure 1. Photo-Reversible, Temperature-Dependent Aggregate Morphologies Induced in Living Cells

(A) Time course of aggregate formation. HeLa cells expressing BA-mGFP were labeled with ReAsH, and both GFP (480 nm, 505 nm dichroic, 535/25 nm; green) and GFP-mediated FRET emission (480 nm, 505 nm dichroic, 653/95 nm; red) channels were collected. GFP quenching and aggregation are complete within approximately 15 min. The scale bars represent 20 μ m.

(B) ReAsH-induced aggregates form as puncta at room temperature. GFP (480/30 nm, 505 nm dichroic, 535/25 nm; green) and ReAsH fluorescence (568/55 nm, 600 nm dichroic, 653/95 nm; red) are overlaid.

(C) ReAsH labeling at 37°C induces the formation of fiber-like aggregates.

(D) Aggregates are dispersed upon spatial ReAsH photobleaching. A defined circular region was exposed to high-intensity excitation light by contracting the microscope objective diaphragm. GFP fluorescence increases and diffuses throughout the cell.

(E) Fiber-like aggregates are also photo-reversible.

larger ribbons (Figure 1C). Both forms of aggregates are stable in cells for days without significant toxicity. Fusion of BA-mGFP to β -lactamase or the protein kinase A pseudosubstrate inhibitor PKI led to the formation of fiber-like aggregates when labeled at room temperature, demonstrating that specific fusion partners can influence the temperature-dependent morphologies. Following a spatially controlled photobleach of either ReAsH or CHOxAsH aggregates, the aggregates dissolved, freeing the fusion protein to diffuse throughout the cell (Figures 1D and 1E). Because of the high concentration of fluorophores present in aggregates, photo-generated free radicals presumably damage neighboring fluorophores, increasing the photobleaching rate of ReAsH by almost an order of magnitude (Figure S5). Photo-induced dispersion of CHOxAsH aggregates requires far less light, as it is approximately two orders of magnitude less photo-stable than ReAsH. Photobleached tetracysteines fail to re-label with fresh biarsenical after dithiol washes, limiting reversible aggregation to one cycle.

To further understand the unique characteristics of this novel reversible aggregation tag, several BA-mGFP fusions were observed using correlated light and electron microscopy. Using the unique functionality of the biarsenical-tetracysteine system, ReAsH fluorescence was photo-oxidized to polymerize diaminobenzidine (DAB) for osmium staining and visualization by electron microscopy (EM) [18]. High-resolution electron micrographs of BA-mGFP labeled at room temperature show small tangles of small fibers radiating from the site of nucleation (Figure 2A). In contrast, BA-mGFP labeled at 37°C aggregates as ordered bundles, aligning the labeled protein into longer fibers (Figure 2B). Several PKA components were readily aggregated upon addition of either CHOxAsH or ReAsH into discrete highly fluorescent puncta. ReAsH aggregates of BA-mGFP-R1 α or BA-mGFP-C α are present as round balls (Figure 2C), approximately the same size as mitochondria, whereas PKI aggregates as long, thick fibers similar to those seen when labeling at 37°C (Figure 2D). The nature of the aggregates are highly variable, but they clearly begin as single fibers of polymerized BA-mGFP that either intertwine or align to form various fiber-like structures.

PKA Holoenzyme Association Visualized by Coaggregation

BA-mGFP-R1 α and BA-mGFP-C α subunits are susceptible to biarsenical-induced aggregation, yet it was unclear whether intact PKA holoenzyme containing both RI and C was recruited to aggregates. Because the excitation peak of CHOxAsH is \sim 100 nm blue-shifted from GFP, both BA-mGFP and mCherry can be visualized without biarsenical excitation or bleaching. Coexpression of BA-mGFP-R1 α and mCherry-C α led to CHOxAsH-dependent coaggregation, demonstrating intact holoenzyme is indeed recruited. Unexpectedly, BA-mGFP-R1 α and mCherry-C α remained colocalized when prestimulated with forskolin, despite persistent cAMP elevation with the phosphodiesterase inhibitor 3-isobutyl-1-methylxanthine (IBMX) (Figure 3A;

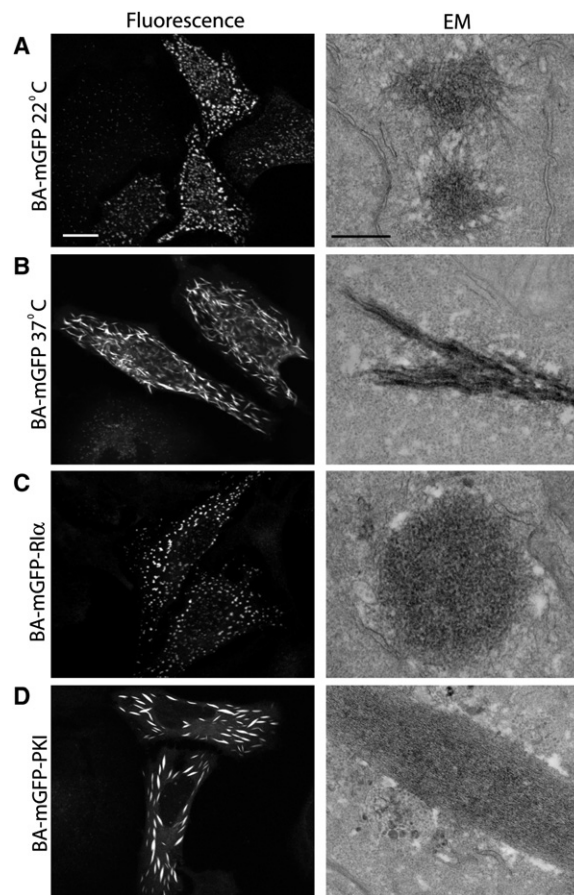


Figure 2. Correlated Light and Electron Microscopy Reveal High-Resolution Aggregate Composition

(A) BA-mGFP labeled with ReAsH at 22°C forms aggregates composed of many small fiber tangles. Individual fibers are seen radiating from the nucleation site. The fluorescence scale bar represents 5 μ m. The EM scale bar represents 500 nm. (B) BA-mGFP labeled with ReAsH at 37°C forms small bunches of fibers. (C) BA-mGFP-R1 α labeled with ReAsH at 22°C forms round, dense aggregates with few radiating fibers. Similar morphology was observed with BA-mGFP-C α aggregates. (D) BA-mGFP-PKI aggregates (22°C) are highly ordered, aligned single fibers that combine to form a large elongated fiber.

Movie S2). This persistent association was not dependent on any specific order or size of fusion tag, as C-terminally tagged C α -HA and C α -mCherry behaved similarly. Likewise, BA-mGFP-C α and mCherry-R1 α also remained associated following stimulation (Figure 3B).

The PKA pseudosubstrate inhibitor PKI binds C α about as strongly as cAMP-free R1 α ($K_d = 0.15$ nM). Both PKI and R1 α are more than simply pseudosubstrate inhibitors, as each has high-affinity binding sites beyond the C α substrate-binding domain. Coexpression of mCherry-PKI showed little effect on R1 α and C α coaggregation in unstimulated, serum-starved cells (Figure 3C), but did prevent coaggregation in forskolin-stimulated cells (Figure 3D). PKI and R1 α compete for a common C α interaction site, and

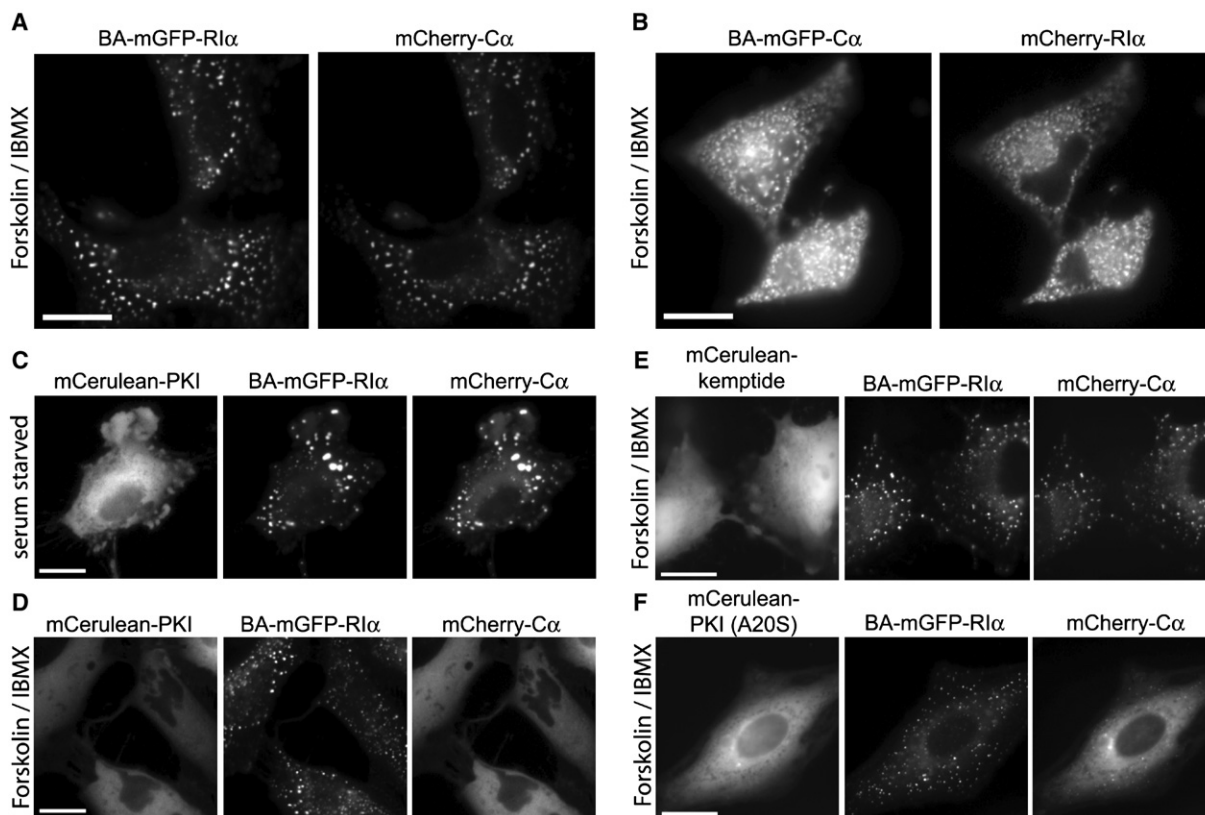


Figure 3. Type I PKA Holoenzyme Coaggregates in Cells

(A) Forskolin stimulation is insufficient to separate BA-mGFP-RI α (480/30 nm, 505 nm dichroic, 535/25 nm) and mCherry-C α (540/25 nm, 560 nm dichroic, 595/50 nm). The scale bars represent 20 μ m.

(B) BA-mGFP-C α and mCherry-Rl α coaggregate despite forskolin stimulation.

(C and D) Coexpression of mCerulean-PKI (436/10 nm, 450 nm dichroic, 460/40 nm) does not disrupt coaggregation of BA-mGFP-RI α and mCherry-C α in serum-starved cells (C), but prevents coaggregation upon the addition of forskolin and IBMX (D).

(E) Expression of mCerulean-kemptide does not disrupt coaggregation in forskolin/IBMX-stimulated cells.

(F) Expression of mCerulean-PKI (A20S) prevents efficient coaggregation in forskolin/IBMX-stimulated cells.

neither BA-mGFP-RI α and mCerulean-PKI or BA-mGFP-PKI and RI α coaggregate. Overexpression of the PKA model substrate mCerulean-kemptide (LRRASLG) (Figure 3E) had no effect on RI α (cAMP) $_2$ and C α coaggregation, but expression of mCerulean-PKI (A20S) (mutated from a pseudosubstrate to a substrate) did block most coaggregation (Figure 3F). Neither substrate was observed in aggregates. Therefore, substrate does not form a stable ternary complex with RI and C, but transiently competes with RI for access to the active site of free C, where it is immediately phosphorylated and released.

Regulatory Inhibitor Domain Regulates C α Coaggregation

There are two general classes of functionally nonredundant PKA regulatory subunits in cells, RI and RII. To understand the dynamics of RII dissociation, we next tested BA-mGFP-RII α and BA-mGFP-RII β in cells, but unfortunately both failed to efficiently aggregate with CHOxAsH. Aggregation may require sufficient linker flexibility, as RI has a flexible 11 residue linker but RII has only 1 or 2 residues

before the dimerization domain. Although we could not directly aggregate RII, CHOxAsH aggregates of BA-mGFP-C α efficiently recruited mCherry-RII α (Figure 4A, upper). In contrast to RI α , mCherry-RII α released from BA-mGFP-C α when stimulated with forskolin alone (Figure 4A, lower). This dissociation occurred exclusively in medium- to low-expressing cells, validating that cAMP raises the dissociation constant of phosphorylated RII holoenzyme to micromolar levels [4]. As was seen with type I PKA, BA-mGFP-C α exchanged mCherry-RII α for mCerulean-PKI only after cAMP stimulation.

A fundamental difference between RI and RII is the sequence of the inhibitor domain that occupies the catalytic site of C α [3]. The inhibitor domain of RI has an alanine at the P site, whereas RII contains a serine, which is autophosphorylated [19]. To determine the importance of the P site residue in RII α , this site was mutated from Ser to Ala. This single mutation blocked cAMP-induced dissociation of mCherry-C α from RII α , even in the presence of mCerulean-PKI (Figure 4B). The analogous Ser-to-Glu mutation slightly affected holoenzyme formation, but

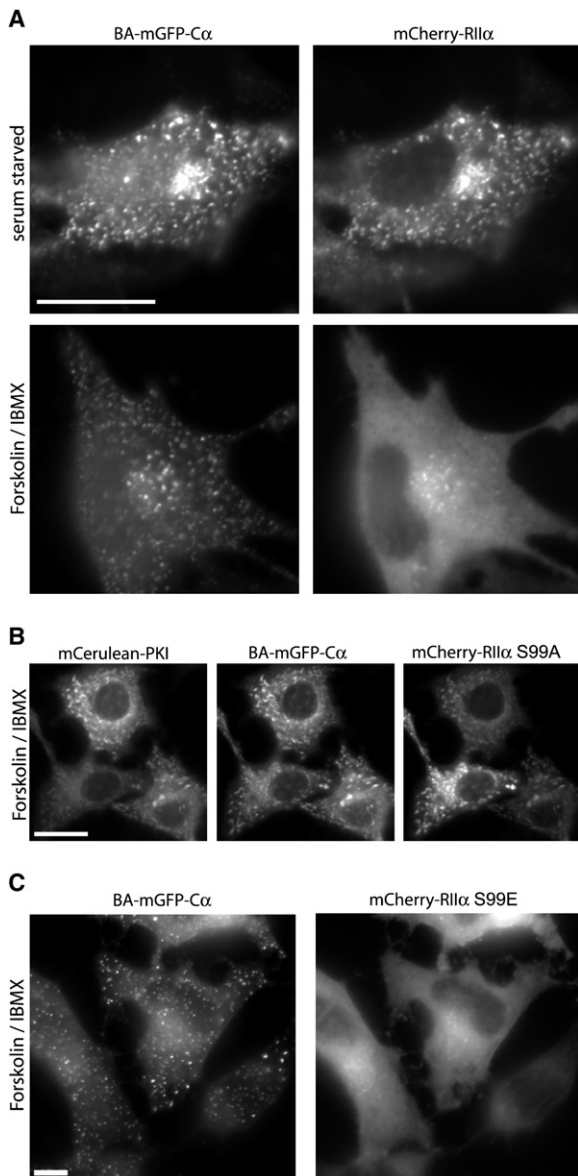


Figure 4. Type II PKA Dissociation Requires Elevated cAMP and Ser-99 Phosphorylation

(A) BA-mGFP- $C\alpha$ (480/30 nm, 505 nm dichroic, 535/25 nm) coaggregates with mCherry-RII α (540/25 nm, 560 nm dichroic, 595/50 nm) in serum-starved cells, but separate following forskolin stimulation in weakly overexpressing cells. The scale bars represent 20 μ m.

(B) Mutation of the RII α inhibitor domain phosphorylation site from Ser to Ala (S99A) blocks dissociation following forskolin stimulation. Coexpression of mCerulean-PKI (436/10 nm, 450 nm dichroic, 460/40 nm) fails to prevent coaggregation of BA-mGFP- $C\alpha$ and mCherry-RII α S99A.

(C) RII α S99E mutation causes forskolin-dependent release of mCherry-RII α from BA-mGFP- $C\alpha$ aggregates.

upon stimulation, $C\alpha$ dissociated in cells expressing even high levels of tagged type II holoenzyme (Figure 4C). In addition, the Glu substitution enhanced $C\alpha$ accessibility for mCerulean-PKI. Phosphorylation of Ser-99 enhances dis-

placement of the RII inhibitor domain, just as other PKA substrates are released after phosphorylation. To block P site phosphorylation by means other than mutation, we pretreated cells with the PKA ATP-binding site inhibitor H89 before raising cAMP. Unexpectedly, H89 not only allowed RII α to dissociate from $C\alpha$ but even promoted dissociation of RII α S99A from $C\alpha$, suggesting additional destabilization of the complex.

Next, we reciprocally mutated the pseudosubstrate sequence of BA-mGFP-RI α to either Ser or Asp, which are known to support intact and cAMP-inducible holoenzyme in vitro [20], albeit with reduced MgATP dependence and increased salt sensitivity. In cells, both mutants still formed holoenzyme, but unlike wild-type BA-mGFP-RI α , each mutation led to cAMP-induced separation in the absence of mCerulean-PKI (Figures 5A and 5B). Under basal conditions, mCerulean-PKI expression alone was sufficient to dissociate BA-mGFP-RI α A97D and in low-expressing BA-mGFP-RI α A97S cells, highlighting the importance of inhibitor displacement for activation. The aggregate density is also affected in BA-mGFP-RI α (A97D), which implies the mutation leads to further conformational changes that weaken aggregation. Altogether, the data presented exemplify a fundamental difference in RI and RII activation and demonstrate how P site phosphorylation of R subunits regulates their ability to release $C\alpha$.

Reversible Inhibition of Nuclear Signaling

In order to understand the functional consequences of intact cAMP-bound type I PKA, we assayed PKA activation in single living cells following forskolin and IBMX addition using the genetically encoded, nuclear-localized, ratio-metric phosphorylation reporter AKAR2-NLS [21]. Coexpression of BA-mGFP- $C\alpha$ and mCherry-RI α led to coaggregation and complete silencing of nuclear PKA activity upon labeling (Figure 6), as BA-mGFP- $C\alpha$ aggregates contain both type I and type II PKA holoenzyme. Low-expressing cells failed to completely inactivate nuclear PKA signaling, presumably because BA-mGFP- $C\alpha$ levels must be sufficient to titrate endogenous $C\alpha$ from native holoenzyme to BA-mGFP- $C\alpha$ hybrid holoenzyme. PKA holoenzyme contains two C subunits and two R subunits, so BA-mGFP- $C\alpha$ aggregates also contain endogenous C subunit recruited in *trans*. By photobleaching ReAsH BA-mGFP- $C\alpha$ aggregates, nuclear activity is restored. These results demonstrate that PKA activity can be inducibly inhibited by biarsenical-dependent aggregation, and reversed by photo-induced reactivation without significant chromophore-assisted light inactivation [22].

AKAP Colocalization Reveals Substrate-Dependent Release

AKAP-mediated targeting of PKA holoenzyme to subcellular locations is a key mechanism for spatially focusing PKA activity [2]. The dual isoform specific DAKAP1 α localizes and concentrates both type I and type II holoenzyme to the outer mitochondrial membrane [23]. Overexpression of this AKAP leads to mitochondrial recruitment and

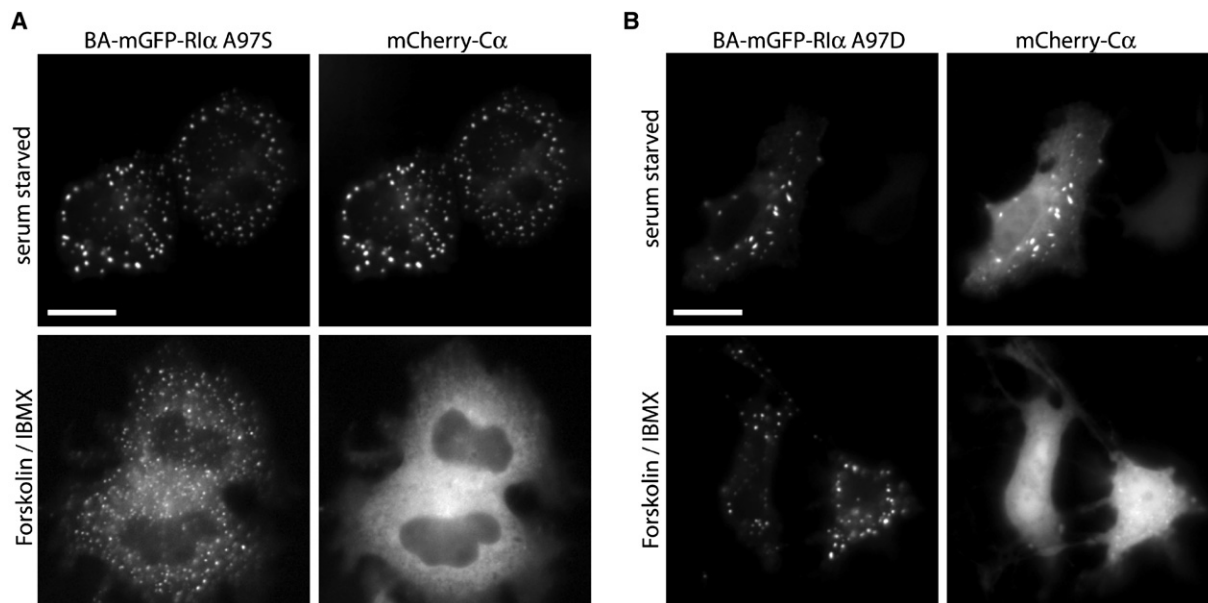


Figure 5. Mutational Analysis of Type I PKA Holoenzyme Dissociation

(A) BA-mGFP-R1 α A97S (495/10 nm, 505 nm dichroic, 535/25 nm) forms intact holoenzyme with mCherry-C α (540/25 nm, 560 nm dichroic, 595/50 nm) in serum-starved cells, but dissociates upon stimulation with forskolin/IBMX. The scale bars represent 20 μ m.

(B) BA-mGFP-R1 α A97D forms holoenzyme with mCherry-C α in serum-starved cells, but dissociates following forskolin/IBMX stimulation.

colocalization of DAKAP1 α -mCerulean, mGFP-R1 α , and mCherry-C α . Importantly, DAKAP1 α localization could alter PKA dynamics by additional endogenous regulatory mechanisms, but because colocalization is not artificially induced, dissociation can be monitored dynamically without potential aggregation-induced artifacts. Following forskolin stimulation, mCherry-C α remained colocalized to DAKAP1 α and R1 α at mitochondria (Figure 7A). As observed with aggregated cytosolic type I holoenzyme, complete dissociation from DAKAP1 α -localized type I holoenzyme only occurred with both forskolin stimulation and coexpression of mCerulean-PKI. Also, similar to type II holoenzyme aggregates, mCherry-C α released from DAKAP1 α -localized mCerulean-R1 α following stimulation, dependent on low expression levels (Figure 7B). Intermediate dissociation was not observed in R1 α -overexpressing cells, suggesting the amount of type II holoenzyme is overcome by R1 α overexpression. Addition of the kemptide-based ratiometric fluorescent reporter AKAR2 had no effect on the separation of DAKAP1 α -localized type I PKA holoenzyme following stimulation. Furthermore, cytosolic kinase activity is significantly reduced by DAKAP1 α localization, correlating with the observed failure to dissociate (Figure 7E). DAKAP1 α localization of type I PKA and expression of AKAR3 fused to the DAKAP targeting motif [24] localizes and concentrates both type I PKA holoenzyme and the reporter substrate. Forskolin and IBMX stimulation led to rapid dissociation of mCherry-C α and a robust kinase response (Figures 7D and 7E), demonstrating localized substrate is required for efficient release of C α from AKAP-localized type I PKA holoenzyme in HeLa cells.

DISCUSSION

By selecting for dithiol-resistant ReAsH-labeled tetracysteine-GFP fusions, we identified a fluorescent tag capable of inducing self-aggregation when labeled with select biarsenical dyes. BA-GFP forms two distinct fiber morphologies dependent on the labeling temperature: puncta at room temperature or fibers at 37°C. Such temperature dependence is reminiscent of the yeast prion protein Sup35, which forms different heritable fiber morphologies dependent on growth temperature [25]. At 4°C, short, fragile, and more infectious prion strains develop, whereas at higher temperatures, longer, more stable, and less infectious prion strains form. We have also observed that certain protein fusions to BA-GFP favor the fiber-like morphology when labeled at room temperature, such as BA-mGFP- β -lactamase and BA-mGFP-PKI. Due to the preferred Pro-Gly sequence internal to the cysteine pairs, we believe the optimal conformation for biarsenical-bound tetracysteines is a β hairpin, similar to the β sheets that define β -amyloid prions. The electron micrographs of BA-GFP show distinct filaments radiating from nucleation sites when labeled at room temperature, and those same fibers become highly ordered when formed at 37°C. More evidence is required to determine the ordering nature of BA-GFP aggregates, but it is intriguing that biarsenical labeling of a unique tetracysteine sequence can induce conformations in GFP that have similarities to protein conformational diseases.

Fusions to the FK506-binding protein (FKBP) and the rapamycin-binding protein (FRB) have found widespread use as a general method for chemically dimerizing

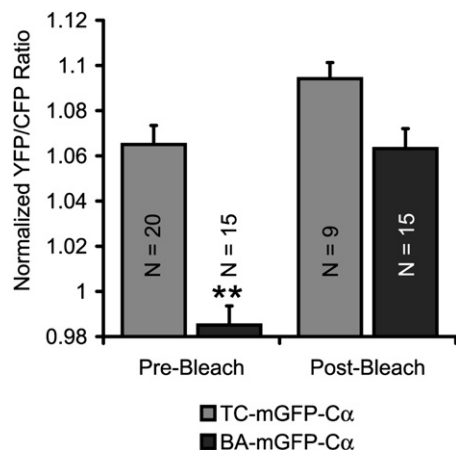


Figure 6. Photo-Reversible Aggregate-Mediated Inactivation of Nuclear PKA

PKA activity was assayed by FRET using nuclear-localized AKAR2, and a time point 30 min after forskolin/IBMX stimulation is shown. BA-mGFP-C α can be reversibly inactivated by ReAsH aggregation ($p = 0.007$). Reactivation by photobleaching ReAsH fully restores nuclear PKA activity. The activity of nonaggregated, ReAsH-labeled TC-mGFP-C α is not significantly affected by photobleaching. Error bars represent standard error values.

engineered proteins in cells upon addition of a divalent ligand [26]. Mutation of F36M in FKBP causes spontaneous homodimerization that reverses upon ligand addition [27]. Four tandem copies of the self-dimerizing F36M mutant of FKBP and one copy of GFP (>75 kDa total) spontaneously crosslink and form large, multiprotein aggregates that are dispersed upon addition of a specific ligand [27], which has proven useful for sequestering proteins in the secretory pathway, such as insulin, for drug-dependent release [28]. Aggregation and dispersion depend on the addition and removal of ligand through incubations and washing steps. BA-GFP may not be as transferable to live animals, but it is smaller (~30 kDa), intrinsically fluorescent, captures weak interaction partners, and is rapidly reversible.

The sequence requirements for C α dissociation from RII α have been visualized in living cells using a novel inducible aggregation tag. CHOxAsH-labeled BA-mGFP-RII α colocalizes in aggregates with mCherry-C α -independent cAMP. Based on stop-flow kinetic measurements, the K_d of cAMP-bound RII α (truncated to remove the dimerization domain) to C α is 130 nM [29], several-fold lower than the estimated cellular PKA concentration of 0.5 μ M [1]. Dimers of the regulatory subunit will likely have a stronger affinity for C α , which will further restrict its diffusion. Therefore, cAMP binding causes a conformational change that weakens type I PKA holoenzyme association but does not permit the majority of C α to visually dissociate at endogenous concentrations [1]. Because BA-GFP requires several micromolar labeled protein to aggregate, we exclusively capture intact holoenzyme. Clearly, RII α (cAMP) $_2$ retains C α nearby until sufficient substrate is present to promote C α diffusion. The pseudosubstrate inhibitor PKI causes visible separation of RII α and C α by trapping C α

and blocking reassociation. Although the binding and kinetic constants of full-length PKI have not been reported, the K_i values of PKI $_{1-24}$, PKI $_{11-30}$ (A20pS), and kemptide are 5 nM, 94 μ M, and 348 μ M, respectively [30, 31]. The K_m for kemptide and PKI $_{14-22}$ (A20S) are 4.7 μ M and 0.11 μ M, respectively [31]. Consequently, due to additional peripheral interactions, the PKI (A20S) is a more efficient substrate than kemptide. Kemptide has also been shown to directly compete with RII α (cAMP) $_2$ for binding C α in vitro [32]. Altogether, by competing for free C α , substrate concentration is critical for allowing C α to diffuse away from RII α . Other mechanisms may also promote diffusion. For example, formation of type I holoenzyme is critically sensitive to ATP and Mg $^{2+}$ concentrations [33], which has been suggested to regulate dissociation in cells. The N terminus of C α also can bind AKIP1 α , a novel A kinase-interacting protein that binds C α and mediates nuclear translocation [34]. Additional posttranslational modifications, such as phosphorylation or myristoylation, could also enhance type I PKA dissociation. Overall, we believe sustained C α dissociation from RII α is likely an orchestrated event that requires highly concentrated substrate and possibly other cell type-dependent mechanisms.

The inhibitor sequence of RII α (RRVS) is a substrate for phosphorylation, whereas the consensus phosphorylation site of RII α (RRGA) contains an alanine at the P site. This fundamental difference changes type II PKA holoenzyme dissociation from substrate regulation to self-regulation by autophosphorylation. Phosphorylation of RII α has been extensively studied and is known to weaken the affinity of cAMP-bound RII α for C α to approximately 6–10 μ M in vitro [35, 36]. This value fits our observations, as we could only see complete dissociation in cells weakly expressing BA-mGFP-C α and mCherry-RII α , in which protein concentrations were probably low μ M. Phosphorylation of RII α is an essential step in C α dissociation, exemplified by inhibition of dissociation by the Ser-to-Ala P site mutation, and the enhanced dissociation by the Ser-to-Glu P site mutation. Overall, colocalization of type II PKA holoenzyme with phosphatases should enhance reassociation by allowing the inhibitor domain to reassociate with C α . Also, because AKAPs concentrate type II PKA holoenzyme to levels approaching the K_d , they may localize activity by decreasing dissociation and diffusion.

AKAPs are known to localize PKA holoenzyme to specific subcellular environments to target specific substrates [2]. Using simple fluorescent protein fusions, we recapitulated our coaggregation results by colocalizing PKA holoenzyme to the surface of mitochondria with DAKAP1 α . RII α failed to release C α upon forskolin stimulation, whereas RII α -bound C α fully dissociated. Based on the K_d of cAMP-bound type I holoenzyme in vitro, it is reasonable to assume that holoenzyme does reassociate when bound to cAMP. Therefore, AKAP tethering could focus kinase activity on a limited pool of substrates while sequestering type I PKA from leaving the local environment, especially after transient physiological stimulation. Interestingly, tethering PKA to the outside of mitochondria reduces the phosphorylation of diffuse substrates. Either AKAR2

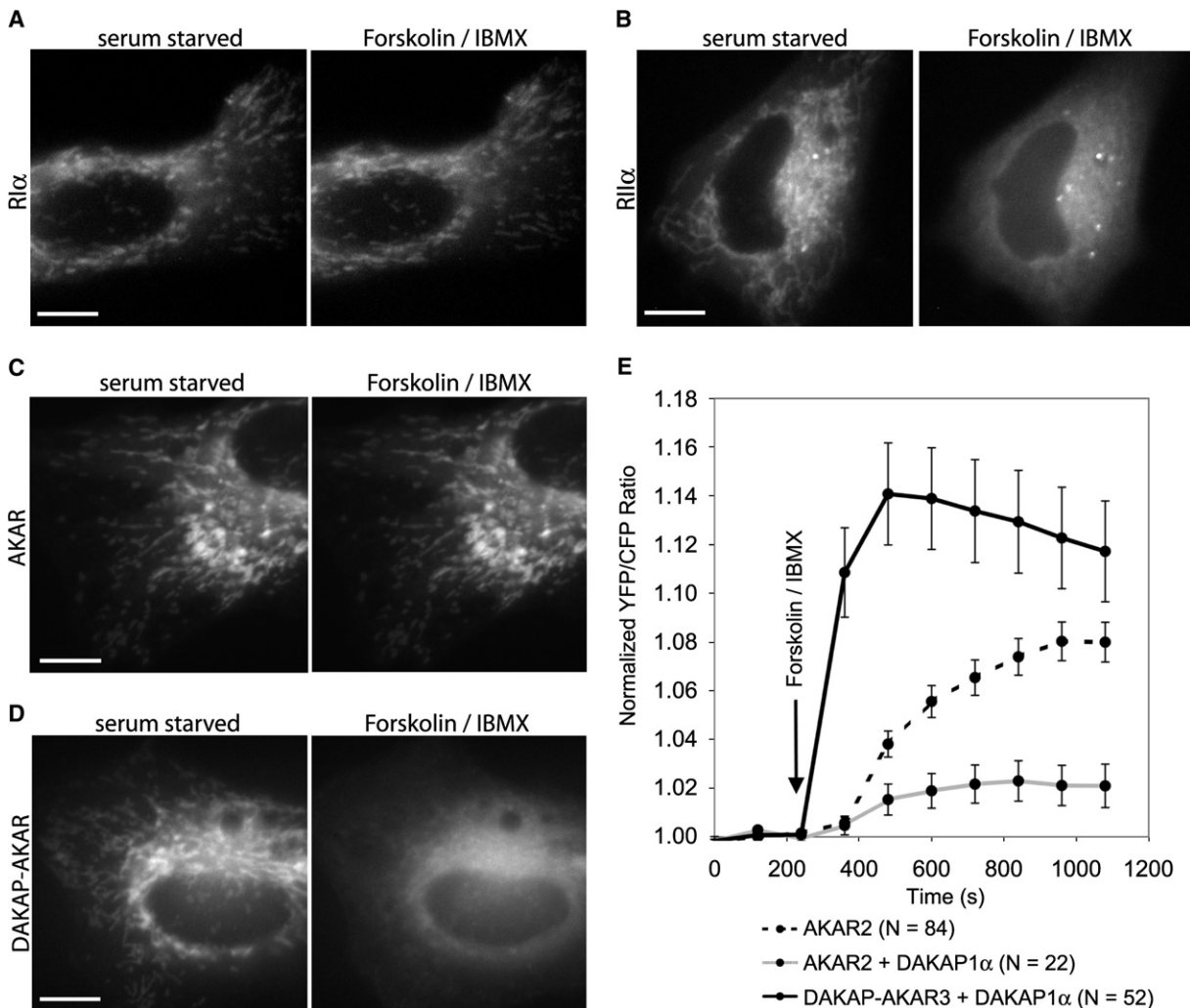


Figure 7. DAKAP1 α Localization and Activity of PKA Isoforms

(A) Cells weakly expressing mGFP-C α (495/10 nm, 505 nm dichroic, 535/25 nm), mCherry-R1 α , and DAKAP1 α -mCerulean localize type I holoenzyme to mitochondria under basal conditions. DAKAP1 α -mCerulean and mCherry-R1 α colocalize to mitochondria with mGFP-C α under all tested conditions (not shown). Forskolin/IBMX stimulation has no effect on mGFP-C α localization as observed 10 min poststimulation in 14 out of 14 cells tested. The scale bars represent 10 μ m.

(B) Type II PKA holoenzyme diffuses from mitochondria following cAMP stimulation. Cells weakly expressing mGFP-C α , mCherry-R1 α , and DAKAP1 α -mCerulean lead to overlap of all three channels under basal conditions. Forskolin/IBMX stimulation led to release of mGFP-C α from mitochondria, specifically in low-expressing cells in 12 out of 12 cells tested.

(C) AKAR2 has no effect on DAKAP1 α -localized type I PKA holoenzyme. Cells coexpressing DAKAP1 α , R1 α , mCherry-C α (580/20 nm, 600 nm dichroic, 653/95 nm), and AKAR2 were imaged. Untargeted AKAR had no effect on type I PKA separation in 15 out of 15 cells tested.

(D) Localized substrate enhances mCherry-C α release from DAKAP1 α localization. Cells coexpressing DAKAP1 α , R1 α , mCherry-C α , and DAKAP-AKAR3 were imaged. Targeting the AKAR3 to the surface of mitochondria with a 15 amino acid DAKAP-targeting motif efficiently colocalizes type I PKA holoenzyme and substrate (not shown), and stimulation causes mCherry-C α release in 18 out of 21 cells tested. The three nondissociated cells have significantly higher expression levels, which led to mitochondrial clumping.

(E) Correlated ratiometric detection of PKA activation demonstrates C α release leads to enhanced kinase activity. We observe less than a 25% increase in the maximal ratio change when comparing AKAR2 to AKAR3. DAKAP1 α localization of type I PKA holoenzyme (red trace) inhibits free cytosolic kinase activity ($p = 5.9 \times 10^{-4}$) compared to untethered holoenzyme (black trace). Colocalizing both type I PKA holoenzyme and the reporter to the surface of mitochondria leads to enhanced kinase activation correlated with mCherry-C α release (green trace). Error bars represent standard error values.

does not have complete access to DAKAP1 α -localized type I PKA, or substrate cannot efficiently compete against concentrated R1 α . In vitro, increasing substrate concentration enhances type I PKA activity [32]. This enhancement is not allosteric, and can be interpreted as

facilitating diffusion from R1 α inhibition. It is paradoxical why C α diffuses away from type II holoenzyme but not type I holoenzyme. R1I is extensively targeted by numerous AKAPs to precise subcellular localizations, whereas R1 is more dynamic and has fewer specific AKAPs.

One solution to this paradox may lie in the composition of the AKAP protein complex. Whereas type I PKA holoenzyme is localized by pseudosubstrate tethering, type II PKA is especially sensitive to phosphatase effects. RII α is known to enhance its affinity to certain AKAPs following S99 phosphorylation [37], but AKAP-dependent changes in C α affinity are not known. DAKAP1 α scaffolds both PKA and PP1 [38], suggesting a biologically important interplay, possibly involving suppression of RII α by PP1-mediated dephosphorylation. AKAP79, an RII-specific AKAP, is colocalized with calcineurin [39], a phosphatase that can dephosphorylate RII. Therefore, one role of PP1 and calcineurin may be to regulate type II PKA activity directly by controlling dissociation and reassociation. Although in our experiments DAKAP1 α -localized RII α failed to retain C α following prolonged cAMP elevation, more physiological cAMP stimulation or coexpression of additional phosphatases may lead to a different outcome. Therefore, AKAPs may prevent C α diffusion by recruiting phosphatases that act to reverse RII α autophosphorylation, thereby effectively tethering C α locally. In future experiments, it will be important to observe coaggregation or colocalization to see whether other RII-specific AKAPs release C α , and whether proteins localized to the AKAP scaffold enhance or inhibit C α diffusion.

In summary, we have characterized BA-GFP as a genetically encoded, dye-dependent reversible aggregator and demonstrated several applications such as induced colocalization and protein inactivation. By applying this technology to study PKA dissociation, we visualized unique requirements that distinguish PKA holoenzyme subtype activation mechanisms in living cells. Our data strongly suggest substrate-mediated regulation of type I PKA, and regulation by autophosphorylation of type II PKA. BA-GFP is ideal for studying weak interactions that change from nanomolar to micromolar affinity in cells, as fluorescent detection generally requires micromolar levels of overexpression. Furthermore, the temperature-dependent morphologies of BA-GFP aggregation are unique, and may be valuable for understanding the mechanism of many pathologically relevant protein-misfolding diseases.

SIGNIFICANCE

Despite decades of research, visualizing PKA activation in cells has been technically challenging and often misleading. Fluorescently tagged regulatory and catalytic PKA subunits can visualize cAMP responses by FRET as a function of conformational changes. Unfortunately, these techniques do not directly demonstrate separation, and only report a change in the distance and orientation of the two chromophores. Although much has been done in vitro to understand the mechanisms of PKA dissociation, the cellular context of C α dissociation of each PKA isoform has not been visualized. The tetracysteine sequence YR-ECCPGCCMWR fused to the N terminus of GFP (BA-GFP) causes rapid protein aggregation upon ReAsH labeling in cells. Fusion of this tag to the N terminus

of various proteins leads to dye-dependent aggregation as temperature-dependent photo-reversible precipitates. Correlated light and electron microscopy reveal that ReAsH-labeled BA-GFP aggregates are composed of disordered BA-GFP polymers that align into larger fibers at higher labeling temperatures. Using the BA-GFP dye-triggered aggregation system, weak interactions between tagged R and C subunits were trapped in highly visible puncta, providing a simple assay to study the mechanisms of C separation. Type I PKA holoenzyme remains intact following maximal cAMP stimulation, whereas type II PKA rapidly dissociates. Targeting PKA holoenzyme to the outside of mitochondria by coexpression of DAKAP1 α confirmed the coaggregation results and demonstrated that type I PKA is only effectively separated by both localized substrate and cAMP stimulation. Overall, type I holoenzyme separation is substrate dependent, whereas type II PKA separation requires autophosphorylation. Additionally, PKA activity can be inhibited by aggregation and restored by biarsenical photo-bleaching. These observations are central to understanding AKAP-mediated targeting, and point to the presence of phosphatases and substrate local concentration as a mechanism for maintaining localization. Furthermore, a novel approach is introduced for visualizing and manipulating protein interactions by dye-dependent aggregation.

EXPERIMENTAL PROCEDURES

Cell Culture and Biarsenical Labeling

HeLa cells were cultured in Dulbecco's modified Eagle's media supplemented with 10% fetal bovine serum, 100 units/ml penicillin G, and 100 μ g/ml streptomycin. Cells were transfected using Fugene HD (Roche) 2 days prior to imaging, and starved in serum-free media overnight. Biarsenical labeling was performed with 1.0 μ M ReAsH or 2.5 μ M CHoXAsH with 10 μ M ethanedithiol (EDT) in Hanks balanced saline solution supplemented with 2 g/l glucose and 20 mM HEPES for 60 min at room temperature or in serum-free media at 37°C. Cyclic AMP was elevated by addition of 10 μ M forskolin (Sigma) and 100 μ M IBMX (Sigma) simultaneous with biarsenical addition. Using purified recombinant standards for normalization by western blot, HeLa cells express endogenous RII α and RII β at relatively equal levels. Biarsenical-stained cells were washed with 0.25 mM 2,3-dimercaptopropanol (BAL) to remove nonspecific ReAsH staining. BA-GFP protein was purified from overexpressing HEK293 cells and labeled in vitro as previously described [13].

Fluorescence Microscopy

Epifluorescence microscopy was performed on a Zeiss Axiovert 200M microscope with a cooled charge-coupled device camera (Roper Scientific) using a computer-controlled MS-2000 (Applied Scientific Instrumentation) automated stage, controlled by METAFUOR 6.1 software (Universal Imaging) or Slidebook 4.1 (Intelligent Imaging Innovations). All imaging experiments were performed at room temperature with a 40 \times 1.3 NA oil objective, sometimes with 2.5 \times optivar magnification for an effective 100 \times magnification. To reverse ReAsH BA-mGFP aggregation, ReAsH was photobleached with 580/20 nm, 0.67 W/cm² for 30 s. Bleached regions were analyzed simultaneously with multiple nonbleached regions in BA-mGFP-RII α and BA-mGFP-C α ReAsH-stained cells.

Correlated Light and Electron Microscopy

ReAsH-labeled cells were fixed in 2% glutaraldehyde in sodium cacodylate buffer (0.1 M, pH 7.4) at 4°C for 20 min. Cells were then rinsed in cacodylate buffer and treated for 5 min with blocking buffer: 10 mM KCN, 10 mM aminotriazole, 0.01% hydrogen peroxide, 50 mM glycine in 0.1 M cacodylate buffer. Images of cells were recorded using a Bio-Rad MRC-1024 confocal system on a Zeiss Axiovert 35M microscope using 568 nm laser excitation and a 63× 1.4 NA objective. The buffer was replaced with oxygenated buffer containing 1 mg/ml DAB, and photoconversion was performed by using intense illumination (75 W xenon lamp without neutral density filters) focused through the microscope objective using a standard rhodamine filter set (535/50 nm, 580 nm dichroic, 590 nm long pass). After a brownish reaction product replaced the fluorescence (8–10 min), the cells were rinsed in cacodylate buffer and postfixed in 2% osmium tetroxide for 1 hr at 4°C. The cells were then dehydrated in ethanol and infiltrated in Durcupan ACM resin (Electron Microscopy Sciences) and polymerized at 60°C. Ultrathin sections were prepared and imaged using a JEOL 1200 electron microscope at 80 keV.

PKA Activity Measurements

Serum-starved HeLa cells expressing AKAR2, AKAR2-NLS, or DAKAP-AKAR3 (420/20 nm, 450 nm dichroic, CFP: 475/40 nm and YFP: 535/25 nm) were imaged every 3 min (unless otherwise noted) and stimulated with 25 μM forskolin and 100 μM IBMX. Twelve or more regions from a single dish were imaged in parallel using a computer-controlled stage. Cells with similar medium levels of AKAR2 or AKAR2-NLS expression were analyzed for each condition and ratios were calculated by dividing background-subtracted YFP-FRET by CFP emission and normalized to basal starting ratio.

Supplemental Data

Supplemental Data include five figures, one table, Supplemental Experimental Procedures, and two movies, and are available at <http://www.chembiol.com/cgi/content/full/14/9/1031/DC1/>.

ACKNOWLEDGMENTS

We wish to acknowledge Stephen Adams, Ben Giepmans, James Lim, Juniper Pennypacker, and Paul Steinbach for helpful advice, discussions, and technical assistance, Yuliang Ma for PKA-related cDNAs, and Jin Zhang (Johns Hopkins University) for DAKAP-AKAR3. Additionally, we would like to thank members of the Tsien and Taylor labs, as well as the FIAshers group for helpful discussions. R.Y.T. is a coinventor on patents assigned to the University of California covering Green Fluorescent Protein mutants, biarsenical dyes, and tetracycline motifs. Support for this work was provided by P41 RR004050 (M.H.E.), NIH DK54441 (S.S.T.), NS27177 (R.Y.T.), GM72033 (R.Y.T.), and the Howard Hughes Medical Institute.

Received: April 2, 2007

Revised: June 28, 2007

Accepted: July 20, 2007

Published: September 21, 2007

REFERENCES

- Kopperud, R., Christensen, A.E., Kjaerland, E., Viste, K., Kleivdal, H., and Doskeland, S.O. (2002). Formation of inactive cAMP-saturated holoenzyme of cAMP-dependent protein kinase under physiological conditions. *J. Biol. Chem.* 277, 13443–13448.
- Wong, W., and Scott, J.D. (2004). AKAP signalling complexes: focal points in space and time. *Nat. Rev. Mol. Cell Biol.* 5, 959–970.
- Kim, C., Vigil, D., Anand, G., and Taylor, S.S. (2006). Structure and dynamics of PKA signaling proteins. *Eur. J. Cell Biol.* 85, 651–654.
- Rubin, C.S., Erlichman, J., and Rosen, O.M. (1972). Molecular forms and subunit composition of a cyclic adenosine 3',5'-monophosphate-dependent protein kinase purified from bovine heart muscle. *J. Biol. Chem.* 247, 36–44.
- Beavo, J.A., Bechtel, P.J., and Krebs, E.G. (1974). Preparation of homogenous cyclic AMP-dependent protein kinase(s) and its subunits from rabbit skeletal muscle. *Methods Enzymol.* 38, 299–308.
- Corbin, J.D., Brostrom, C.O., Alexander, R.L., and Krebs, E.G. (1972). Adenosine 3',5'-monophosphate-dependent protein kinase from adipose tissue. *J. Biol. Chem.* 247, 3736–3743.
- Adams, S.R., Harootunian, A.T., Buechler, Y.J., Taylor, S.S., and Tsien, R.Y. (1991). Fluorescence ratio imaging of cyclic AMP in single cells. *Nature* 349, 694–697.
- Adams, S.R., Bacskai, B.J., Taylor, S.S., and Tsien, R.Y. (1999). Optical probes for cAMP. In *Fluorescent and Luminescent Probes for Biological Activity*, W.T. Mason, ed. (London: Academic Press), pp. 156–172.
- Zaccolo, M., De Giorgi, F., Cho, C.Y., Feng, L., Knapp, T., Negulescu, P.A., Taylor, S.S., Tsien, R.Y., and Pozzan, T. (2000). A genetically encoded, fluorescent indicator for cyclic AMP in living cells. *Nat. Cell Biol.* 2, 25–29.
- Prinz, A., Diskar, M., Erlbruch, A., and Herberg, F.W. (2006). Novel, isotype-specific sensors for protein kinase A subunit interaction based on bioluminescence resonance energy transfer (BRET). *Cell. Signal.* 18, 1616–1625.
- Yang, S., Fletcher, W.H., and Johnson, D.A. (1995). Regulation of cAMP-dependent protein kinase: enzyme activation without dissociation. *Biochemistry* 34, 6267–6271.
- Vigil, D., Blumenthal, D.K., Brown, S., Taylor, S.S., and Trewella, J. (2004). Differential effects of substrate on type I and type II PKA holoenzyme dissociation. *Biochemistry* 43, 5629–5636.
- Martin, B.R., Giepmans, B.N.G., Adams, S.R., and Tsien, R.Y. (2005). Mammalian cell-based optimization of the biarsenical-binding tetracycline motif for improved fluorescence and affinity. *Nat. Biotechnol.* 23, 1308–1314.
- Cubitt, A.B., Woollenweber, L.A., and Heim, R. (1999). Understanding structure-function relationships in the *Aequorea victoria* green fluorescent protein. *Methods Cell Biol.* 58, 19–30.
- Adams, S.R., Campbell, R.E., Gross, L.A., Martin, B.R., Walkup, G.K., Yao, Y., Llopis, J., and Tsien, R.Y. (2002). New biarsenical ligands and tetracycline motifs for protein labeling in vitro and in vivo: synthesis and biological applications. *J. Am. Chem. Soc.* 124, 6063–6076.
- Griffin, B.A., Adams, S.R., and Tsien, R.Y. (1998). Specific covalent labeling of recombinant protein molecules inside live cells. *Science* 281, 269–272.
- Zacharias, D.A., Violin, J.D., Newton, A.C., and Tsien, R.Y. (2002). Partitioning of lipid-modified monomeric GFPs into membrane microdomains of live cells. *Science* 296, 913–916.
- Gaietta, G., Deerinck, T.J., Adams, S.R., Bouwer, J., Tour, O., Laird, D.W., Sosinsky, G.E., Tsien, R.Y., and Ellisman, M.H. (2002). Multicolor and electron microscopic imaging of connexin trafficking. *Science* 296, 503–507.
- Rangel-Aldao, R., and Rosen, O.M. (1976). Mechanism of self-phosphorylation of adenosine 3':5'-monophosphate-dependent protein kinase from bovine cardiac muscle. *J. Biol. Chem.* 251, 7526–7529.
- Durgerian, S., and Taylor, S.S. (1989). The consequences of introducing an autophosphorylation site into the type I regulatory subunit of cAMP-dependent protein kinase. *J. Biol. Chem.* 264, 9807–9813.
- Zhang, J., Hupfeld, C.J., Taylor, S.S., Olefsky, J.M., and Tsien, R.Y. (2005). Insulin disrupts β-adrenergic signalling to protein kinase A in adipocytes. *Nature* 437, 569–573.

22. Tour, O., Meijer, R.M., Zacharias, D.A., Adams, S.R., and Tsien, R.Y. (2003). Genetically targeted chromophore-assisted light inactivation. *Nat. Biotechnol.* *21*, 1505–1508.
23. Huang, L.J.S., Durick, K., Weiner, J.A., Chun, J., and Taylor, S.S. (1997). Identification of a novel protein kinase A anchoring protein that binds both type I and type II regulatory subunits. *J. Biol. Chem.* *272*, 8057–8064.
24. Allen, M.D., and Zhang, J. (2006). Subcellular dynamics of protein kinase A activity visualized by FRET-based reporters. *Biochem. Biophys. Res. Commun.* *348*, 716–721.
25. Tanaka, M., Collins, S.R., Toyama, B.H., and Weissman, J.S. (2006). The physical basis of how prion conformations determine strain phenotypes. *Nature* *442*, 585–589.
26. Clemons, P.A. (1999). Design and discovery of protein dimerizers. *Curr. Opin. Chem. Biol.* *3*, 112–115.
27. Rollins, C.T., Rivera, V.M., Woolfson, D.N., Keenan, T., Hatada, M., Adams, S.E., Andrade, L.J., Yaeger, D., van Schravendijk, M.R., Holt, D.A., et al. (2000). A ligand-reversible dimerization system for controlling protein-protein interactions. *Proc. Natl. Acad. Sci. USA* *97*, 7096–7101.
28. Rivera, V.M., Wang, X., Wardwell, S., Courage, N.L., Volchuk, A., Keenan, T., Holt, D.A., Gilman, M., Orci, L., Cerasoli, F., Jr., et al. (2000). Regulation of protein secretion through controlled aggregation in the endoplasmic reticulum. *Science* *287*, 826–830.
29. Anand, G., Taylor, S.S., and Johnson, D.A. (2007). Cyclic-AMP and pseudosubstrate effects on type-I A-kinase regulatory and catalytic subunit binding kinetics. *Biochemistry* *46*, 9283–9291.
30. Scott, J.D., Glaccum, M.B., Fischer, E.H., and Krebs, E.G. (1986). Primary-structure requirements for inhibition by the heat-stable inhibitor of the cAMP-dependent protein kinase. *Proc. Natl. Acad. Sci. USA* *83*, 1613–1616.
31. Glass, D.B., Cheng, H.C., Mende-Mueller, L., Reed, J., and Walsh, D.A. (1989). Primary structural determinants essential for potent inhibition of cAMP-dependent protein kinase by inhibitory peptides corresponding to the active portion of the heat-stable inhibitor protein. *J. Biol. Chem.* *264*, 8802–8810.
32. Viste, K., Kopperud, R.K., Christensen, A.E., and Doskeland, S.O. (2005). Substrate enhances the sensitivity of type I protein kinase A to cAMP. *J. Biol. Chem.* *280*, 13279–13284.
33. Herberg, F.W., and Taylor, S.S. (1993). Physiological inhibitors of the catalytic subunit of cAMP-dependent protein kinase: effect of magnesium-ATP on protein-protein interactions. *Biochemistry* *32*, 14015–14022.
34. Sastri, M., Barraclough, D.M., Carmichael, P.T., and Taylor, S.S. (2005). A-kinase-interacting protein localizes protein kinase A in the nucleus. *Proc. Natl. Acad. Sci. USA* *102*, 349–354.
35. Doskeland, S.O., Maronde, E., and Gjertsen, B.T. (1993). The genetic subtypes of cAMP-dependent protein kinase—functionally different or redundant? *Biochim. Biophys. Acta* *1178*, 249–258.
36. Granot, J., Mildvan, A.S., Hiyama, K., Kondo, H., and Kaiser, E.T. (1980). Magnetic resonance studies of the effect of the regulatory subunit on metal and substrate binding to the catalytic subunit of bovine heart protein kinase. *J. Biol. Chem.* *255*, 4569–4573.
37. Zakhary, D.R., Moravec, C.S., and Bond, M. (2000). Regulation of PKA binding to AKAPs in the heart: alterations in human heart failure. *Circulation* *101*, 1459–1464.
38. Steen, R.L., Martins, S.B., Tasken, K., and Collas, P. (2000). Recruitment of protein phosphatase 1 to the nuclear envelope by A-kinase anchoring protein AKAP149 is a prerequisite for nuclear lamina assembly. *J. Cell Biol.* *150*, 1251–1261.
39. Klauck, T.M., Faux, M.C., Labudda, K., Langeberg, L.K., Jaken, S., and Scott, J.D. (1996). Coordination of three signaling enzymes by AKAP79, a mammalian scaffold protein. *Science* *271*, 1589–1592.